

# Continuous Localization of Ventricular Tachycardia Exit Sites in Patients With Previous Myocardial Infarction

Potse M.<sup>1</sup>, Linnenbank A. C.<sup>1</sup>, SippensGroenewegen A.<sup>2</sup>, and Grimbergen C. A.<sup>1</sup>

<sup>1</sup>Academic Medical Center, Amsterdam, The Netherlands;

<sup>2</sup>Cardiac Focus Inc., Pleasanton CA, USA.

## Introduction

Ventricular tachycardia (VT) occurring late after myocardial infarction may be treated curatively with catheter ablation using radiofrequency energy. For successful ablation the tip of the catheter must be accurately positioned in the critical part of the VT reentrant circuit. Identifying the arrhythmia substrate using traditional catheter mapping techniques is time consuming since it requires sequential sampling of activation times during VT from the entire left ventricle.

The procedure may be shortened by utilizing body surface mapping to quickly identify the target area by first determining the exit site of the VT, from where a suitable ablation site can be found by a short local activation sequence mapping procedure [1]. A database of paced body surface QRS integral maps (QRSI's) corresponding to known pacing positions is helpful for localization of the VT exit site. Because an infarction scar influences the relation between QRSI and exit site, specific databases have been developed for patients with a normal left ventricle (NLV) and with prior inferior (IMI) or anterior myocardial infarction (AMI) [2, 3]. With these databases, localization can be performed by identifying one of 18 to 25 segments in the left ventricle. To increase localization accuracy, an algorithm was previously developed that provides continuous localization by interpolating in the NLV database [4]. We adapted this algorithm to render it suitable for the AMI and IMI databases as well, and tested it with all three databases. Adaptation was necessary to accommodate the somewhat more irregular distribution of exit site coordinates over QRSI space that was observed in AMI and IMI patients.

## Method

The endocardial wall is described using "left ventricular cylinder coordinates" [2]. These coordinates are based on the line from the LV apex to the geometric middle of the mitral valve ring. The *ventricular length*  $\ell$  is the distance of a position, projected on this axis, to the apex, and normalized to the axis length; the *ventricular angle*  $\alpha$  is the angle of a position relative to the angle of the aortic valve ring (AVR). Figure 1 illustrates these concepts.

Pace mapping data from the studies of SippensGroenewegen et al. were used to train and test our method [2, 3]. To create the databases, these authors recorded 62-lead body surface electrocardiograms during LV pace mapping

in patients. The position of the catheter tip was determined quantitatively using digitized biplane X-ray images, with a localization error of at most 7 mm [2]. These paced maps are used here to fit and test our algorithm.

Onset and offset of the QRS interval, and suitable time instants for baseline correction were selected manually according to previously defined criteria [2]. A linear correction for baseline drift was applied. The QRS integral map was computed by summing each lead over the QRS interval, and then interpolating the irregularly spaced sites to a regular  $12 \times 16$  matrix. In the interpolation process, faulty leads were replaced by interpolated values in the same way as the non-measured grid points. For further analysis, we used the 192-element maps; this was done to work with a more universal electrode array; we could also have used the 62 leads with interpolated rejected leads.

A complete description of the algorithm was previously given [4]. The modified algorithm is presented here briefly. A QRSI is regarded as a 192-element vector, containing an element corresponding to each of the  $12 \times 16$  grid points. A fixed Karhunen–Loève transform, previously determined

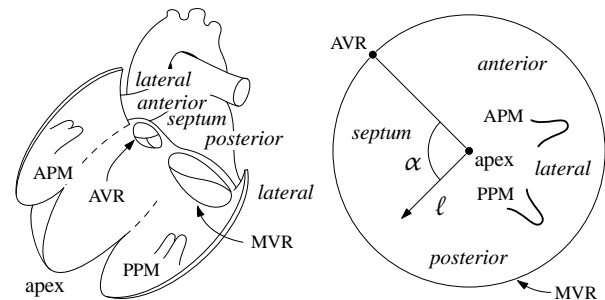


**Fig. 1:** Schematic anatomic diagram (left) [5, 6] and polar projection of the left ventricle (right) [2]. The circumference of the diagram represents approximately the mitral valve ring (MVR); the position of the aortic valve ring (AVR) is indicated. The positions of the anterior and posterior papillary muscles (APM and PPM) and endocardial quadrants (septum, anterior, lateral, and posterior) are indicated in both diagrams. The diagram also illustrates the left ventricular cylinder coordinates which are employed here. These coordinates consist of a relative length  $\ell$ , indicating the distance along the apex–MVR axis relative to the distance from apex to MVR, and an azimuth  $\alpha$ , defined with respect to the position of the AVR.

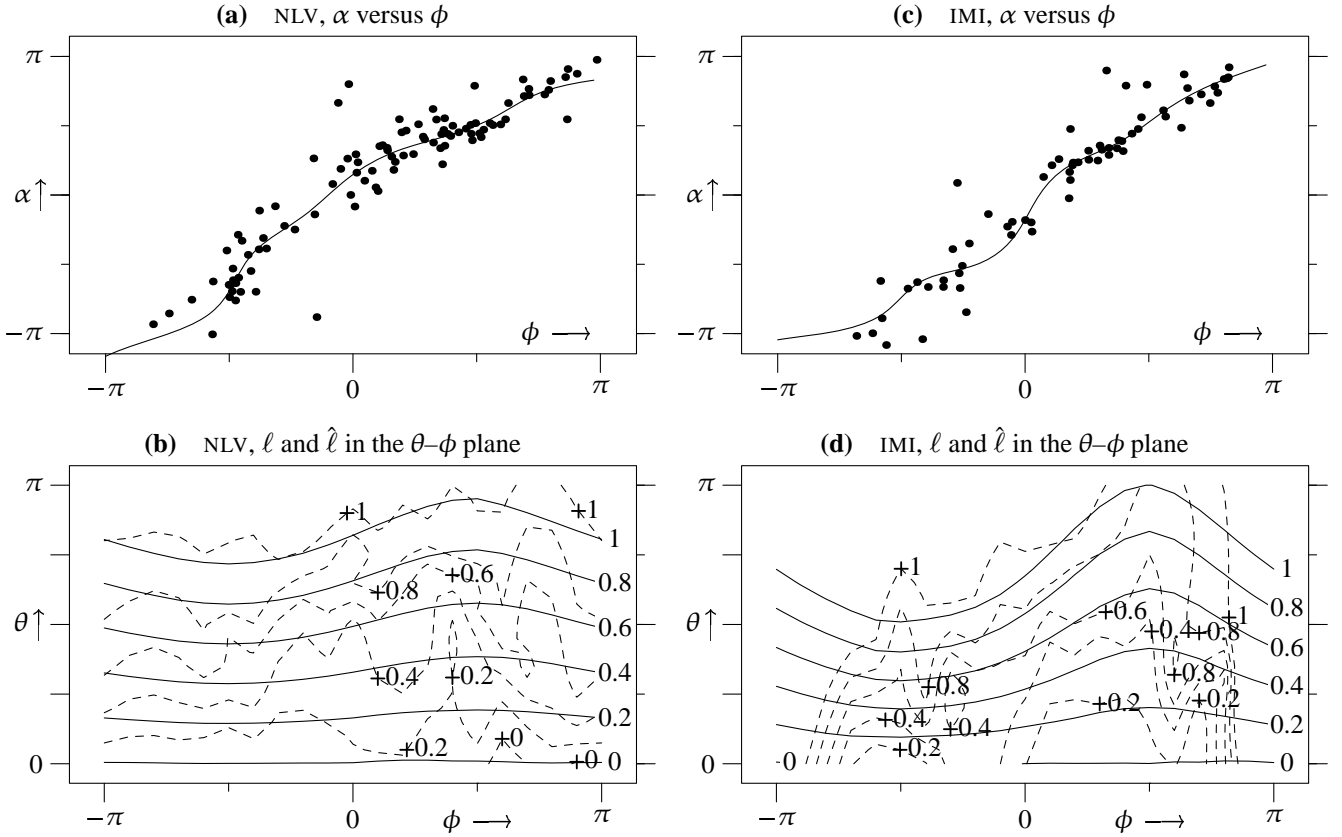


**Fig. 2:** (a) Measured coordinate  $\alpha$  of the NLV database of 99 paced maps shown with dots versus the map coordinate  $\phi$ . The solid line represents the spline estimate for  $\hat{\alpha}$ , fitted to the database. (b) Measured coordinate  $\ell$  of the NLV database, interpolated in the  $\theta$ - $\phi$  plane, shown with dashed contour lines; these contour lines are labeled with “plus” signs. Also shown, with solid contour lines, labeled on the right side of the plot, is the estimate  $\hat{\ell}$  computed with equation (3), fitted to the database. (c) Measured and estimated  $\alpha$  coordinate of the IMI database of 66 paced maps, displayed analogously to (a). (d) Measured an estimated  $\ell$  coordinate of the IMI database, displayed analogously to (b).

from a large set of BSM data, was applied to each QRSI: the covariance between the 192 channels of the data set was computed, and the eigenvectors  $\vec{\psi}_i$  of the covariance matrix were determined using MATLAB software (The MathWorks Inc.). Then each QRSI  $\vec{m}$  was expressed in terms of these (orthonormal) eigenvectors, as

$$\vec{m} = \sum_{i=1}^{192} w_i \vec{\psi}_i, \quad (1)$$

where

$$w_i = \vec{m} \cdot \vec{\psi}_i. \quad (2)$$

We found that the first three coefficients  $w_i$ , which correspond to the three  $\vec{\psi}_i$  with the largest eigenvalues, describe at least 90% ( $97 \pm 2\%$ ) of the energy content of  $\vec{m}$ , that is,  $(w_1^2 + w_2^2 + w_3^2)/|\vec{m}| > 0.9$  for each  $\vec{m}$  [4].

The coefficients  $w_1$ ,  $w_2$ , and  $w_3$  of each map  $\vec{m}$  were treated as Cartesian coordinates in a 3-D space and expressed in spherical coordinates  $r$ ,  $\theta$ , and  $\phi$ , and the other 189 coefficients were discarded. The axis of the spherical coordinate system was chosen such that a database QRSI corresponding approximately to the LV apex had  $\theta = 0$ . The radius  $r$  is an estimate of the total energy content of

the map, and was also discarded. The surface in QRSI space described by the  $\theta$  and  $\phi$  coordinates could then be mapped to the LV endocardial surface.

A position on the LV wall is denoted with a pair  $(\ell, \alpha)$ , where  $\ell$  stands for the ventricular length and  $\alpha$  represents the ventricular angle (see Fig. 1). Estimated coordinates are indicated as  $\hat{\ell}$  and  $\hat{\alpha}$ . We observed that the parameter  $\theta$  of a QRSI corresponded approximately to the ventricular length  $\ell$  of the site of origin, and  $\phi$  corresponded approximately to the ventricular angle  $\alpha$ . This is partly a result of our definition that  $\theta = 0$  in the apex. The relationship between the pairs  $(\theta, \phi)$  and  $(\ell, \alpha)$  is illustrated in Fig. 2.

Figure 2 (b) shows, for the NLV database, that  $\ell$  depends primarily on  $\theta$ , with a small contribution of  $\phi$ , which can be approximated by adding a sine wave contribution that is slightly larger for higher values of  $\theta$ . We devised the following function to relate  $\ell$  to  $\theta$  and  $\phi$ :

$$\hat{\ell} = [d_4 + \theta] [d_1 + d_2 \sin(\phi - d_3)] / \pi \quad (3)$$

Figure 2 (a) shows that the relation between  $\alpha$  and  $\phi$  is almost linear for the NLV database; Fig. 2 (c) shows that the relation is more complicated in the IMI database. Therefore the  $\alpha$  coordinate was modeled as a function of  $\phi$  using a spline curve with  $N_c$  control points  $(\phi_i, c_i)$ . It turned out that  $N_c = 11$  was the smallest value that could be chosen

**Table 1:** Localization errors obtained by applying an algorithm trained with each of the three databases to each database in turn. The number of patients and the total number of paced maps included in each database are also indicated.

training set	nr. of patients	nr. of maps	mean (s.d.) error in mm for testing set:		
			NLV	AMI	IMI
NLV	8	99	<b>12 (7)</b>	16 (10)	17 (12)
AMI	8	92	16 (8)	<b>15 (10)</b>	19 (11)
IMI	4	66	16 (11)	21 (11)	<b>12 (11)</b>

for the number of vertices without increasing the average localization error. The parameters  $c_i$  and  $d_i$  were obtained by fitting the model to the database maps. The resulting functions  $\hat{\alpha}$  and  $\hat{\ell}$  for the NLV and IMI databases are shown with solid lines in Fig. 2. Results for the AMI database are not shown; these were similar to the NLV results.

## Results

Localization errors were computed by projecting the localization result, which is given in LV cylinder coordinates, on a triangulated model of the ventricular wall. The model was scaled such that the length of the axis from the apex to the geometric middle of the mitral valve ring was 80 mm. Localization differences could then be expressed as 3-D distances in millimeters, in order to provide an indication of the resolution of the algorithm.

Training and testing were performed using the same sets of paced maps. In order to obtain a representative and unbiased estimate of the error that the algorithm will make if applied to new maps, we used cross-validation: the fitting procedure for  $c_i$  and  $d_i$  was applied to all but one of the database maps, the localization error of the omitted map was computed, and this procedure was repeated leaving out every map in turn.

Each database consisted of 66–99 paced maps with known pacing positions [3]. The algorithm was trained with each database in turn, and then tested with all databases. Estimated localization errors are given in Table 1.

When the appropriate algorithm is used, average errors range from  $12 \pm 7$  mm for the NLV database to  $15 \pm 10$  mm for the AMI database.

## Discussion

As expected, an algorithm specifically trained for a database performs best for that database. In addition, the NLV algorithm performs reasonably for all three databases, and clearly better than the IMI algorithm performs for the AMI test set and the AMI algorithm for the IMI test set.

The results indicate that: (1) The algorithm works well for all three databases, with localization errors in the order of 15 mm. These errors may be largely attributable to

uncertainty in the catheter position data (max. 7 mm) and inter-patient variability. (2) Specific training of the algorithm was more useful for the IMI database than for the AMI database: when using the NLV algorithm the average error was 16 mm for AMI and 17 mm for IMI; with specific algorithms this reduced to 15 mm for AMI and 12 mm for IMI, that is an improvement of 1 mm and 5 mm, respectively. This difference may be due to a larger inter-patient variability in the AMI group. (3) An algorithm fitted to AMI to localize in an IMI patient or vice versa has a larger error than an algorithm fitted to NLV, which suggests that the effects of AMI and IMI on the relation between exit site and QRSI pattern are (in part) opposite.

Applicability to patients with other types of infarction, such as lateral myocardial infarction, has not been tested since there was not enough data available for them [3].

## References

- [1] Peeters, H. A. P., SippensGroenewegen, A., Wever, E. F. D., Rammanna, H., Linnenbank, A. C., Potse, M., Grimbergen, C. A., van Hemel, N. M., Hauer, R. N. W., and Robles de Medina, E. O. Clinical application of an integrated 3-phase mapping technique for localization of the site of origin of idiopathic ventricular tachycardia. *Circulation*, 99:1300–1311, March 1999.
- [2] SippensGroenewegen, A., Spekhorst, H., van Hemel, N. M., Kingma, J. H., Hauer, R. N. W., Janse, M. J., and Dunning, A. J. Body surface mapping of ectopic left and right ventricular activation: QRS spectrum in patients without structural heart disease. *Circulation*, 82:879–896, 1990.
- [3] SippensGroenewegen, A., Spekhorst, H., van Hemel, N. M., Kingma, J. H., Hauer, R. N. W., Janse, M. J., and Dunning, A. J. Body surface mapping of ectopic left ventricular activation: QRS spectrum in patients with prior myocardial infarction. *Circ. Res.*, 71(6):1361–1378, 1992.
- [4] Potse, M., Linnenbank, A. C., Peeters, H. A. P., SippensGroenewegen, A., and Grimbergen, C. A. Continuous localization of cardiac activation sites using a database of multichannel ECG recordings. *IEEE Trans. Biomed. Eng.*, 47(5):682–689, May 2000.
- [5] Josephson, M. E., Horowitz, L. N., Spielman, S. R., Waxman, H. L., and Greenspan, A. M. Role of catheter mapping in the preoperative evaluation of ventricular tachycardia. *Am. J. Cardiol.*, 49:207–220, January 1982.
- [6] Cassidy, D. M., Vassallo, J. A., Buxton, A. E., Doherty, J. U., Marchlinski, F. E., and Josephson, M. E. The value of catheter mapping during sinus rhythm to localize site of origin of ventricular tachycardia. *Circulation*, 69(6):1103–1110, June 1984.